Letter

Transient ordering in the Gross-Pitaevskii lattice after an energy quench within a nonordered phase

Andrei E. Tarkhov,[1,*] A. V. Rozhkov,[2] and Boris V. Fine[3,†]

[1]*Division of Genetics, Department of Medicine, Brigham and Women's Hospital and Harvard Medical School, Boston, Massachusetts 02115, USA*

[2]*Institute for Theoretical and Applied Electrodynamics, Russian Academy of Sciences, Moscow 125412, Russia*

[3]*Institute for Theoretical Physics, University of Leipzig, Brüderstrasse 16, 04103 Leipzig, Germany*

(Received 27 August 2021; revised 18 October 2022; accepted 24 October 2022; published 17 November 2022)

We numerically investigate heating-and-cooling quenches taking place entirely in the nonordered phase of the discrete Gross-Pitaevskii equation on a three-dimensional cubic lattice. In equilibrium, this system exhibits a $U(1)$-ordering phase transition at an energy density which is significantly lower than the minimum one during the quench. Yet, we observe that the postquench relaxation is accompanied by a transient $U(1)$ ordering, namely, the correlation length of $U(1)$ fluctuations significantly exceeds its equilibrium prequench value. The longer and the stronger the heating stage of the quench, the stronger is the $U(1)$ transient ordering. We identify the origin of this ordering with the emergence of a small group of slowly relaxing lattice sites accumulating a large fraction of the total energy of the system. Our findings suggest that the transient ordering may be a robust feature of a broad class of physical systems. This premise is consistent with the growing experimental evidence of the transient $U(1)$ order in rather dissimilar settings.

DOI: 10.1103/PhysRevB.106.L201110

Introduction. The response of an interacting many-body system to a sudden change of external conditions, a quench, has recently become a subject of intense experimental and theoretical research [1–16]. Thermalization after a quench may take a very long time [7,16] and exhibit a rich variety of transient regimes [1–7,15–21]. It can also be accompanied by the spontaneous formation of inhomogeneous structures [7,10], the latter being regularly discussed in numerous papers dedicated, among other topics, to superconducting, charge ordering, and magnetic transitions. There is also mounting experimental evidence [1–7] that a large variety of many-body systems may exhibit nontrivial transient ordering in response to a quench. The proposed interpretations of the nonequilibrium transient order revival/enhancement [7,17,21] are often based on the notion of multiple orders competing against each other both thermodynamically and kinetically.

In this Letter, we show that, quite surprisingly, a very simple theoretical model with a single ordered phase is sufficient for observing the transient ordering. We numerically simulate the discrete Gross-Pitaevskii equation (DGPE) on a three-dimensional (3D) lattice, which exhibits an equilibrium phase transition below a certain temperature. In Fig. 1, we sketch the transient ordering of the system in the process of quenching. During the quench, the system is subjected to fast heating followed by fast cooling which ultimately brings the energy back to the prequench value. It is worth noting that before, during, and after the quench the energy remains within the high-temperature nonordered phase on the phase diagram. Yet, we observe that the transient order, absent in equilibrium, emerges during the quench, and persists long after that. We argue that the mechanism behind the observed transient ordering involves the emergence of a small number of lattice sites with an atypically high concentration of energy. These sites are the 3D counterparts of the so-called discrete breathers that are shown to slow down thermalization in 1D DGPE chains [22–31]. Their concentration may be as little as several percent, yet they pull a significant fraction of total energy from the rest of the system, thereby temporarily cooling the latter, which in turn leads to the detected transient order. Below, we present a detailed description of our simulations, substantiate our conclusions about the transient ordering mechanism, and, finally, discuss the implications of our findings.

The model. The DGPE system on a 3D cubic lattice is a classical dynamical system describing evolution of complex variables $\psi_j(t)$ by the following equations,

$$i\frac{d\psi_j}{dt} = -\sum_{m\in \mathrm{NN}(j)} \psi_m + g|\psi_j|^2\psi_j, \tag{1}$$

where g is the interaction parameter, indices j and m label sites of the underlying 3D lattice, and notation $\mathrm{NN}(j)$ refers to all sites that are nearest neighbors to site j. The DGPE conserves total energy $E = E^{(\mathrm{kin})} + E^{(\mathrm{pot})}$, where the kinetic energy is $E^{(\mathrm{kin})} = -\sum_j \sum_{m\in \mathrm{NN}(j)} \psi_m^*\psi_j$, and the potential energy is $E^{(\mathrm{pot})} = \frac{g}{2}\sum_j |\psi_j|^4$. The norm (also called the "total number of particles") $N = \sum_j n_j = \sum_j |\psi_j|^2$ is another integral of motion associated with the invariance of Eq. (1) relative to the global "gauge transformation" $\psi_j \to e^{i\alpha}\psi_j$. In this work, we fix $g = 10$ and $N = V$, where V is the total number of sites ($V = 50 \times 50 \times 50$). The energy density, $\varepsilon = E/V - g/2$, is the only parameter that is being changed in the process of quenching.

*atarkhov@bwh.harvard.edu

†boris.fine@uni-leipzig.de

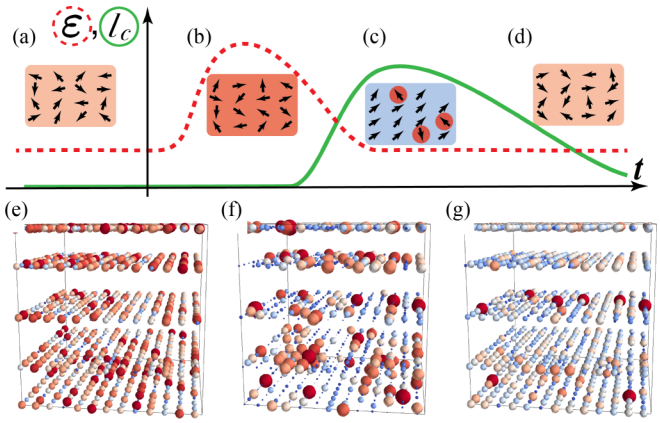

FIG. 1. Sketch of the quench procedure. The quench starts at $t = 0$. The system energy (dashed red line) initially grows, then it reverts to the prequench value. Due to a high prequench energy density, the correlation length (green line) is small before the quench, then grows rapidly due to the quench, relaxing back to the initial value after a long relaxation period. The cartoons (a)–(d) depict internal system states at different stages of the quench. The color represents local energy density, with dark blue being the lowest, and bright red being the highest, and the arrows correspond to the DGPE complex variables ψ_j. The equilibrium state, with moderately high energy density and vanishing correlation length, is shown in (a), (d), and (e). The hot midquench state is in (b) and (f). Transient ordering is visualized in (c) and (g): The arrow directions are ordered, the energy density is inhomogeneous, with lumps of high energy shown by red color, and the rest of the system being significantly cooler. (e)–(g) Visualization of the DGPE simulation. Local values of n_j are shown by volume and color of the balls: Blue (red) represents "cold" ("hot") sites.

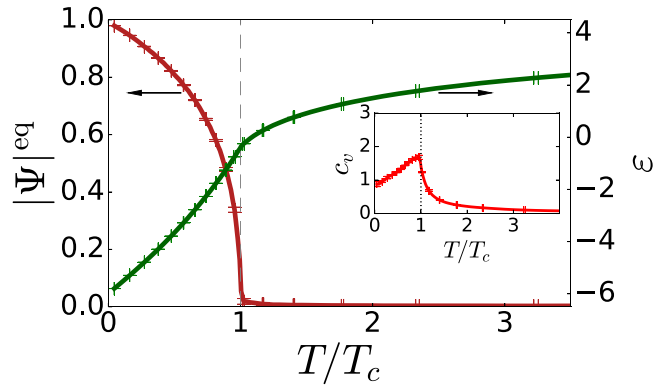

FIG. 2. Temperature dependence of the energy density ε, order parameter $|\Psi|^{eq}$, and the specific heat c_v (inset).

Equilibrium state of DGPE system. For sufficiently large lattice sizes and generic initial conditions the DGPE dynamics is chaotic, and exhibits ergodization that has been checked by various numerical ergodicity tests [32–36]. The averaged dynamics may be characterized in terms of entropy and temperature [37] within microcanonical thermodynamic formalism [38–42]. In equilibrium the microcanonical temperature T and ε are connected by a monotonically growing invertible function $\varepsilon = \varepsilon^{eq}(T)$. This function, evaluated numerically and shown in Fig. 2 for $g = 10$, displays an inflection point accompanied by a corner of the specific heat, $c_v \equiv d\varepsilon(T)/dT$, at $T_c \approx 4.25$. It is associated with the transition into a low-temperature ordered state, characterized by the $U(1)$ order parameter $\Psi(t) = |\Psi(t)|e^{i\phi(t)} = \frac{1}{V}\sum_j \psi_j(t)$. The equilibrium order parameter $|\Psi| = |\Psi|^{eq}(T)$ is a decreasing function of T for $T < T_c$, vanishing above T_c.

We also define the correlation length l_c of the $U(1)$ order as the characteristic length of the decay of the correlation function $\langle\psi_m^*\psi_j\rangle$. The specific definition is $l_c \equiv 1/\Delta k$, where Δk is the half width at half maximum for the Fourier-spectrum intensity $|\psi(\mathbf{k})|^2$ around the peak at the wave vector $\mathbf{k} = \mathbf{0}$ [37]. This peak has a finite width above T_c, implying that l_c has a finite value, which increases as T decreases towards T_c.

Transient ordering. Before the quench, the system is prepared in an equilibrium state in a nonordered phase at temperature $T_0 > T_c$. Then, the system is subjected to a fast energy increase followed by a cooling step, which brings the energy back to its prequench value. This is achieved by introducing a time-dependent "gauge-invariant" term $-K\psi_j D_j$ into the right-hand side of Eq. (1). Here, $D_j = i\sum_{m\in NN(j)}(\psi_m^*\psi_j - \psi_m\psi_j^*)$, and the real function $K = K(t,\kappa)$ is designed [37] to guarantee that the total energy grows initially but later returns to the prequench value. Parameter κ controls the quench strength [37]. Our quench term directly changes only the kinetic energy of the system, but this change then quickly affects the potential energy through the system's dynamics.

Our main results for various quenches starting from equilibrium at temperature $T_0 = 2.3T_c$ are presented in Fig. 3, where Fig. 3(a1) shows the correlation length $l_c(t)$ for a family of shorter quenches of varying strength, while Fig. 3(b1) does the same for a family of longer quenches. The profiles of the quenches are shown in the insets of Figs. 3(a2) and 3(b2), respectively. When $t < 0$, $l_c \approx 3$ in units of the lattice period. Once a quench is launched at $t = 0$, the system energy spikes, and the correlation length initially decreases during the heating stage, but then starts growing during the cooling stage, reaching the maximum around the end of the cooling and then very slowly relaxing back to the equilibrium value. The maximum value of $l_c(t)$ for the shorter quenches is a factor of three larger than the equilibrium one. For longer quenches the increase of $l_c(t)$ is even more significant, but here the maximum of l_c is limited by the size of the simulated lattice ($V = 50 \times 50 \times 50$), which means that it would be even larger in the thermodynamic limit. Overall, the above phenomenology means that the local $U(1)$ ordering exhibits a large long-lived transient increase. We also note that the longer quenches lead to a significantly longer lifetime of the transient order than the shorter ones.

The origin of the transient ordering. Our analysis indicates that the observed transient ordering is caused by the emergence of a small number of "hot" lattice sites that have an anomalously large norm $|\psi_j|^2$ and thus carry even more anomalous local potential energy $\frac{g}{2}|\psi_j|^4$—see the sketch in Fig. 1. While comprising only a small percentage of all lattice sites, the hot sites trap a significant fraction of the total energy deposited into the system during the initial stage of the quench. At the same time, these sites become largely

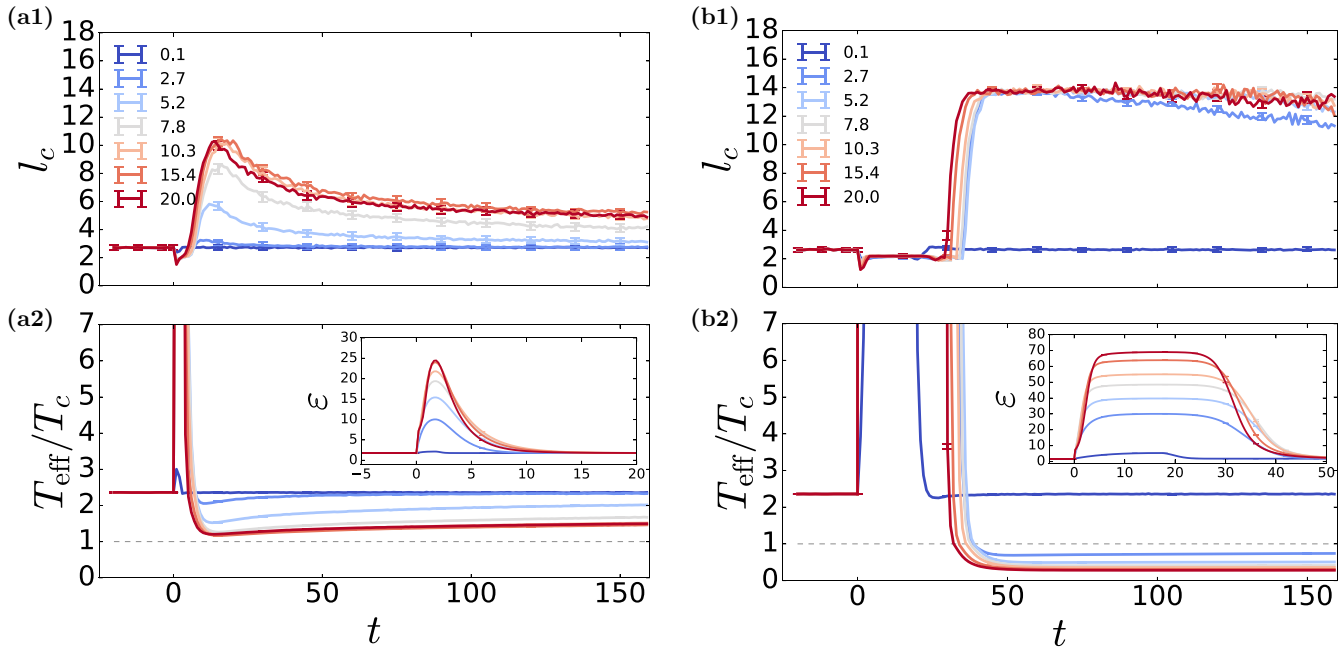

FIG. 3. Correlation length $l_c(t)$ of transient $U(1)$ ordering for shorter quenches (a1) and longer quenches (b1). The quench strength parameter κ is given in the plot legends. (a2), (b2) The effective temperature $T_{\rm eff}(t)$ for cold sites corresponding to (a1) and (b1), respectively. The gray dashed line indicates $T_{\rm eff} = T_c$. In (a2), $T_{\rm eff}$ stays above T_c but comes close to it. In (b2), $T_{\rm eff}$ drops significantly below T_c. Insets of (a2) and (b2): Energy density $\varepsilon(t)$ during the quenches.

decoupled from the rest of the system after the quench and thus relax very slowly [37]. Since after the quench the total energy of the system returns to the initial value, the trapping of the energy by the hot sites implies that the energy density after the quench for the rest of the system must become smaller than the initial energy density. As a result, the effective temperature after the quench for the part of the system excluding hot sites becomes lower than the initial one. This lower effective temperature gets closer to the ordering temperature T_c and may even become lower than T_c as was the case for our longer quenches.

To substantiate the above explanation, we examine the histograms of local potential energies $\varepsilon_j^{(\rm pot)} = \frac{g}{2}|\psi_j|^4$ as functions of time. These histograms in equilibrium and at two different moments of time after a quench are presented in Fig. 4. While comparing equilibrium and nonequilibrium histograms, one notices the salient enhancement of the number of sites with very high values of the potential energy in far-from-equilibrium states. Energy does not spread evenly over the whole system, but instead preferably accumulates on a few sites.

In order to formally divide the system into "hot" and "cold" sites, we introduce a cutoff for the on-site potential energy $\varepsilon_{\rm th} \gg E/V$: Any site j, for which the potential energy $\varepsilon_j^{(\rm pot)} \equiv \frac{g}{2}|\psi_j|^4 > \varepsilon_{\rm th}$, is considered hot, otherwise, it is cold. We set $\varepsilon_{\rm th} = 100$. With such a choice, the percentage of hot sites $x_{\rm hot}$ for our prequench equilibrium state at $T_0 \approx 2.3T_c$ is nearly zero, and so is their total potential energy $E_{\rm hot}^{(\rm pot)}$. The quench acts to increase both $x_{\rm hot}$ and $E_{\rm hot}^{(\rm pot)}$. For the state represented in Fig. 4(c), one has $x_{\rm hot} \approx 0.5\%$ and $E_{\rm hot}^{(\rm pot)}/E \approx 0.7$. As a result, the energy density of cold sites drops significantly below the initial energy density ε. Since the fraction of hot sites $x_{\rm hot}$ is minuscule, the ensemble of the cold sites essentially coincides with the whole system.

To demonstrate the overcooling of the cold sites, we monitor their effective temperature $T_{\rm eff}$. As "a thermometer" for the cold subsystem, we use the kinetic energy density of the cold sites obtained as $\varepsilon_{\rm cold}^{(\rm kin)}(t) = \frac{E^{(\rm kin)}(t) - E_{\rm hot}^{(\rm kin)}(t)}{(1-x_{\rm hot})V}$, where $E^{(\rm kin)}$ is the total kinetic energy of the lattice and $E_{\rm hot}^{(\rm kin)}$ is the part involving the hot sites. The values of $\varepsilon_{\rm cold}^{(\rm kin)}$ are then converted into $T_{\rm eff}$ using the computed equilibrium plot of temperature as a function of $\varepsilon^{(\rm kin)}$ given in the Supplemental Material [37]. The resulting dependence $T_{\rm eff}(t)$ is presented in Figs. 3(a2) and 3(b2). As expected, one sees there that, for both shorter and longer quenches, $l_c(t)$ grows as $T_{\rm eff}(t)$ decreases towards T_c, which indicates that the transient ordering originates from the overcooling of the cold part of the system.

Discussion and conclusions. The DGPE on a sufficiently large lattice cluster represents a very simple model of a microcanonical thermodynamic system exhibiting a phase transition into a $U(1)$-ordered phase. If a time-dependent perturbation, representing external drive, is included, one can use the DGPE to study nonequilibrium dynamics near the continuous transition. The model is characterized by the following three features: (i) In equilibrium, the model has a single ordered phase; (ii) by the model's very design, postquench dynamics is inseparable from equilibrium state properties, as both are governed by the same set of differential equations; and (iii) all equilibrium and postquench properties are controlled entirely by the energy density ε and the interaction parameter g. Points (i)–(iii) imply that very little room for fine tuning is available for the DGPE. Despite that, however, the model demonstrates a robust transient ordering, which is a remarkable nonequilibrium phenomenon.

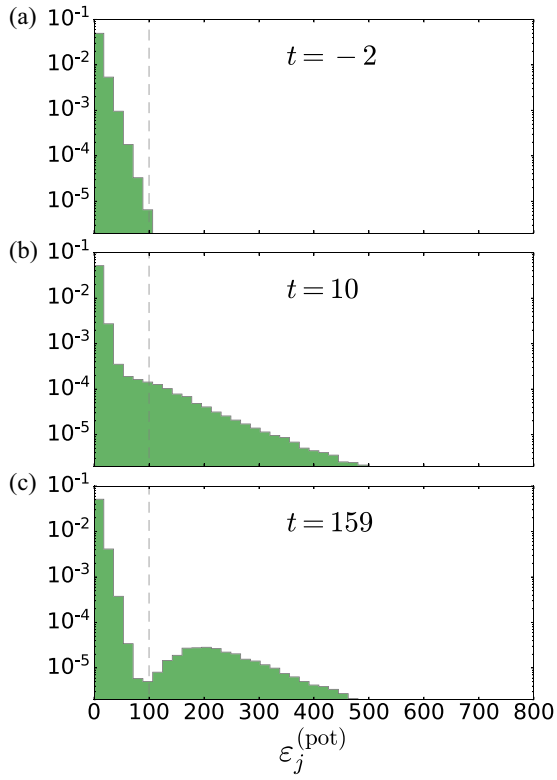

FIG. 4. Histograms of local potential energies $\varepsilon_j^{(\mathrm{pot})} = \frac{g}{2}|\psi_j|^4$ corresponding to the shorter quench in Figs. 3(a1) and 3(a2) with $\kappa = 20$. (a) Equilibrium distribution. (b) Distribution immediately after the quench ($t = 10$). (c) Distribution during the postquench relaxation ($t = 160$). The horizontal axis represents local potential energy, and the vertical axis shows the fraction of sites with a given value of $\varepsilon_j^{(\mathrm{pot})}$. The presence of a larger number of sites with atypically large potential energy is visible in (b) and (c). The threshold energy $\varepsilon_{\mathrm{th}} = 100$ is marked by vertical dashed lines.

In the simulations, the transient ordering manifested itself as a dramatic increase of the phase coherence length l_c. This increase persists much longer than the duration of the quench; its relaxation is then remarkably sluggish [see Figs. 3(a1) and 3(b1)]—a consequence of the long lifetime of the hot sites. The emergence of hot sites is the property of the high-energy regime of DGPE, which is known to exhibit poorly ergodizing dynamics. Reaching high energies of the DGPE lattice necessarily requires the potential energy of the system to become high, but this is only possible when the distribution of norm $|\psi_j|^2$ becomes highly inhomogeneous, thereby facilitating the large energy contribution $\frac{g}{2}|\psi_j|^4$ from the hot sites. The strong energy quench just takes the system into that poorly ergodizing regime, and then the hot sites remain "stuck" in that regime after the energy density of the system returns to the initial value.

We remark in this regard that the strength of the quench in the present investigation is significantly larger than in our closely related work [43], where the focus was on investigating vorticity around the phase transition temperature, hence the quenches did not reach the poorly ergodizing regime. Another comment is that our numerical implementation of the quench was based on pumping the kinetic energy associated with the terms $\psi_m^*\psi_j$. This procedure is uniform throughout the system, and then the hot sites arise dynamically. We suppose that the transient ordering would also be achieved by pumping the potential energy, but making the potential energy very high is only possible by distributing the norm $|\psi_j|^2$ nonuniformly, which would introduce an additional arbitrary element into our simulations.

The experimental context of our simulations extends to physical systems exhibiting phase transitions associated with $U(1)$ ordering. These, in particular, include superfluid and superconducting systems, systems exhibiting density-wave orders, and also magnetically ordered systems with easy-plane anisotropy. One can coarse-grain these systems into parts that are smaller than the expected length of the $U(1)$ phase coherence and yet large enough to justify the classical modeling of each coarse-grained element. Each variable ψ_j of our modeled lattice would then be associated with the average $U(1)$ order within one coarse-grained element (see, e.g., Ref. [43]). The quench can be implemented in solid-state systems either by fast heating of the system by a laser pulse, followed by fast cooling of the excited degrees of freedom by a much larger heat reservoir, or by laser-induced temporary modification of the parameters of the effective time-averaged Hamiltonian for the relevant degrees of freedom.

Several cases of the transient $U(1)$ ordering have already been reported in the literature [1–5]. Particularly relevant here are the observations in the alkali-doped fulleride superconductor K_3C_{60} [5]. The system there was excited at temperatures significantly above the superconducting T_c, and then not only a superconductinglike response was observed as such, but also its lifetime has become dramatically longer once the duration of the laser pulse increased. In other words, a longer pulse resulted in a stronger low-temperature-like response, which is reproduced by our simulations [compare shorter quenches in Figs. 3(a1) and 3(a2) to longer quenches in Figs. 3(b1) and 3(b2)]. Although modeling of a real superconducting system based on DGPE is a rather oversimplified approach, it is difficult to ignore the remarkable parallels between the above experiment and our simulations. In the simulations, the attainment of the transient ordering required us to pump a lot of energy into the system to reach the regime, where the potential energy can no longer be uniformly distributed over the lattice, which, in turn, led to poorly ergodized dynamics characterized by the long-living hot sites. This suggests a generic mechanism of transient ordering in real systems, namely, (i) a quench brings the system into a poorly ergodizing regime, and then (ii) the ordering emerges as a consequence of the dynamical memory of that regime. We note that the long life of the hot DGPE sites is simply a consequence of their dynamical decoupling from the "cold" sites. Such a behavior can be reasonably expected not only for the on-site potential energy of the form prescribed by DGPE but also for a broader class of potential energies, e.g., the capacitive potential energy terms for superconducting islands. Furthermore, if the $U(1)$ ordering transition in a superconducting system is due to the Josephson coupling between superconducting islands, then the primary action of the laser pulse may be not in heating the phase degrees of freedom but rather in renormalizing down the effective Josephson coupling. In terms of the DGPE

modeling, this would mean the reduction of the prefactor of the kinetic energy $E^{(\mathrm{kin})}$. (That prefactor was equal to 1 in our simulations.) Such a change would reduce the ratio of T_c to the total energy density (including the potential energy), which, in turn, would correspond to the nonergodic regime described above.

Our treatment of transient coherence can be compared with alternative ways of theoretical modeling of light-induced phase coherence. We note in this regard that the long life of the superconducting response in the experiment of Ref. [5] after the end of the laser pulse is a challenge for the theoretical approaches explaining the laser-induced superconductivity by a periodic driving of the electron-phonon system [44–51]. Whether the long-lived transient coherence can be explained using explicitly dissipative modeling, such as done, e.g., in Refs. [5,52], is yet to be seen.

To conclude, we numerically studied the nonequilibrium evolution of the 3D DGPE model subjected to an energy quench. Transient $U(1)$ ordering was consistently observed, provided that the quench was strong enough. We explain this phenomenon in terms of long-living hot breatherlike lattice sites possessing anomalously large potential energies. Such nonequilibrium behavior may be an intrinsic feature of a broad class of dynamical models. Our findings may, in particular, shed light on the experimental observations of the transient ordering in superconducting and charge-density-wave systems.

The code is publicly available in a GitHub repository [53].

Acknowledgments. This work was supported in part by a grant of the Russian Science Foundation (Project No. 17-12-01587).

[1] D. Fausti, R. I. Tobey, N. Dean, S. Kaiser, A. Dienst, M. C. Hoffmann, S. Pyon, T. Takayama, H. Takagi, and A. Cavalleri, Science **331**, 189 (2011).
[2] C. R. Hunt, D. Nicoletti, S. Kaiser, T. Takayama, H. Takagi, and A. Cavalleri, Phys. Rev. B **91**, 020505(R) (2015).
[3] M. Mitrano, A. Cantaluppi, D. Nicoletti, S. Kaiser, A. Perucchi, S. Lupi, P. Di Pietro, D. Pontiroli, M. Riccó, S. R. Clark, D. Jaksch, and A. Cavalleri, Nature (London) **530**, 461 (2016).
[4] A. Cantaluppi, M. Buzzi, G. Jotzu, D. Nicoletti, M. Mitrano, D. Pontiroli, M. Riccó, A. Perucchi, P. Di Pietro, and A. Cavalleri, Nat. Phys. **14**, 837 (2018).
[5] M. Budden, T. Gebert, M. Buzzi, G. Jotzu, E. Wang, T. Matsuyama, G. Meier, Y. Laplace, D. Pontiroli, M. Riccó, F. Schlawin, D. Jaksch, and A. Cavalleri, Nat. Phys. **17**, 611 (2021).
[6] J. Zhou and L. Hsiung, J. Mater. Res. **21**, 904 (2006).
[7] A. Kogar, A. Zong, P. E. Dolgirev, X. Shen, J. Straquadine, Y.-Q. Bie, X. Wang, T. Rohwer, I.-C. Tung, Y. Yang, R. Li, J. Yang, S. Weathersby, S. Park, M. E. Kozina, E. J. Sie, H. Wen, P. Jarillo-Herrero, I. R. Fisher, X. Wang *et al.*, Nat. Phys. **16**, 159 (2020).
[8] A. Zong, X. Shen, A. Kogar, L. Ye, C. Marks, D. Chowdhury, T. Rohwer, B. Freelon, S. Weathersby, R. Li, J. Yang, J. Checkelsky, X. Wang, and N. Gedik, Sci. Adv. **4**, eaau5501 (2018).
[9] A. Zong, P. E. Dolgirev, A. Kogar, E. Ergeçen, M. B. Yilmaz, Y.-Q. Bie, T. Rohwer, I.-C. Tung, J. Straquadine, X. Wang, Y. Yang, X. Shen, R. Li, J. Yang, S. Park, M. C. Hoffmann, B. K. Ofori-Okai, M. E. Kozina, H. Wen, X. Wang *et al.*, Phys. Rev. Lett. **123**, 097601 (2019).
[10] A. Zong, A. Kogar, Y.-Q. Bie, T. Rohwer, C. Lee, E. Baldini, E. Ergeçen, M. B. Yilmaz, B. Freelon, E. J. Sie, H. Zhou, J. Straquadine, P. Walmsley, P. E. Dolgirev, A. V. Rozhkov, I. R. Fisher, P. Jarillo-Herrero, B. V. Fine, and N. Gedik, Nat. Phys. **15**, 27 (2019).
[11] R. Yusupov, T. Mertelj, V. V. Kabanov, S. Brazovskii, P. Kusar, J.-H. Chu, I. R. Fisher, and D. Mihailovic, Nat. Phys. **6**, 681 (2010).
[12] M. Collura and F. H. L. Essler, Phys. Rev. B **101**, 041110(R) (2020).
[13] Y. Lemonik and A. Mitra, Phys. Rev. B **98**, 214514 (2018).
[14] Z. Sun and A. J. Millis, Phys. Rev. B **101**, 224305 (2020).
[15] P. E. Dolgirev, A. V. Rozhkov, A. Zong, A. Kogar, N. Gedik, and B. V. Fine, Phys. Rev. B **101**, 054203 (2020).
[16] P. E. Dolgirev, M. H. Michael, A. Zong, N. Gedik, and E. Demler, Phys. Rev. B **101**, 174306 (2020).
[17] J. Ni and B. Gu, Phys. Rev. Lett. **79**, 3922 (1997).
[18] J. Ni and B. Gu, J. Phys.: Condens. Matter **10**, 3523 (1998).
[19] H. Gilhøj, C. Jeppesen, and O. G. Mouritsen, Phys. Rev. Lett. **75**, 3305 (1995).
[20] X. Zhang and M. H. F. Sluiter, Phys. Rev. Mater. **3**, 095601 (2019).
[21] Z. Sun and A. J. Millis, Phys. Rev. X **10**, 021028 (2020).
[22] T. Dauxois and M. Peyrard, Phys. Rev. Lett. **70**, 3935 (1993).
[23] R. S. MacKay and S. Aubry, Nonlinearity **7**, 1623 (1994).
[24] S. Flach and C. Willis, Phys. Rep. **295**, 181 (1998).
[25] D. K. Campbell, S. Flach, and Y. S. Kivshar, Phys. Today **57** (1), 43 (2004).
[26] B. Rumpf, Phys. Rev. E **69**, 016618 (2004).
[27] M. Ivanchenko, O. Kanakov, V. Shalfeev, and S. Flach, Physica D **198**, 120 (2004).
[28] S. Flach and A. V. Gorbach, Phys. Rep. **467**, 1 (2008).
[29] B. Rumpf, Phys. Rev. E **77**, 036606 (2008).
[30] B. Rumpf, Physica D **238**, 2067 (2009).
[31] Y. Kati, Equilibrium and non-equilibrium Gross-Pitaevskii lattice dynamics: Interactions, disorder, and thermalization, Ph.D. thesis, Center for Theoretical Physics of Complex Systems, Institute for Basic Science, 2021.
[32] A. E. Tarkhov, S. Wimberger, and B. V. Fine, Phys. Rev. A **96**, 023624 (2017).
[33] A. E. Tarkhov and B. V. Fine, New J. Phys. **20**, 123021 (2018).
[34] T. Mithun, Y. Kati, C. Danieli, and S. Flach, Phys. Rev. Lett. **120**, 184101 (2018).
[35] A. Y. Cherny, T. Engl, and S. Flach, Phys. Rev. A **99**, 023603 (2019).
[36] A. E. Tarkhov, Ergodization dynamics of the Gross-Pitaevskii equation on a lattice, Ph.D. thesis, Skolkovo Institute of Science and Technology, 2020.
[37] See Supplemental Material at http://link.aps.org/supplemental/10.1103/PhysRevB.106.L201110 for details of the microcanonical properties of DGPE; energy quench; correlation length

and finite-size effects; "hot" sites: additional characterization; equilibrium kinetic energy density as a measure of the system's temperature; transient ordering in a small cluster; and emergence of $U(1)$ order for longer quenches in large systems.

[38] H. H. Rugh, Phys. Rev. Lett. **78**, 772 (1997).

[39] H. H. Rugh, J. Phys. A: Math. Gen. **31**, 7761 (1998).

[40] W. K. den Otter and W. J. Briels, J. Chem. Phys. **109**, 4139 (1998).

[41] W. K. den Otter and W. J. Briels, J. Chem. Phys. **112**, 7283 (2000).

[42] A. S. de Wijn, B. Hess, and B. V. Fine, Phys. Rev. E **92**, 062929 (2015).

[43] A. E. Tarkhov, A. V. Rozhkov, and B. V. Fine, Phys. Rev. B **106**, L121109 (2022).

[44] Z. M. Raines, V. Stanev, and V. M. Galitski, Phys. Rev. B **91**, 184506 (2015).

[45] R. Höppner, B. Zhu, T. Rexin, A. Cavalleri, and L. Mathey, Phys. Rev. B **91**, 104507 (2015).

[46] S. J. Denny, S. R. Clark, Y. Laplace, A. Cavalleri, and D. Jaksch, Phys. Rev. Lett. **114**, 137001 (2015).

[47] A. Komnik and M. Thorwart, Eur. Phys. J. B **89**, 244 (2016).

[48] Y. Murakami, N. Tsuji, M. Eckstein, and P. Werner, Phys. Rev. B **96**, 045125 (2017).

[49] D. M. Kennes, E. Y. Wilner, D. R. Reichman, and A. J. Millis, Nat. Phys. **13**, 479 (2017).

[50] M. Babadi, M. Knap, I. Martin, G. Refael, and E. Demler, Phys. Rev. B **96**, 014512 (2017).

[51] Z. Dai and P. A. Lee, Phys. Rev. B **104**, 054512 (2021).

[52] P. E. Dolgirev, A. Zong, M. H. Michael, J. B. Curtis, D. Podolsky, A. Cavalleri, and E. Demler, Commun. Phys. **5**, 234 (2022).

[53] https://github.com/TarkhovAndrei/DGPE.